2023-01-1381

Icing Qualification Wind Tunnel Test of Helicopter Engine with Inlet Barrier Filter Air Intake

Stefan van ‘t Hoff and Karel Lammers
Royal Netherlands Aerospace Centre (NLR)

Joo Hyun Jung and Hyung Sik Kim
Korea Aerospace Industries, Ltd.

Sandy Ressejac
Safran Helicopter Engines

Abstract

Icing wind tunnel testing was performed as part of the Republic of Korea certification of the Light Civil Helicopter (LCH) for inadvertent flight in icing conditions. The test was aimed at the compliance demonstration of the engine and air intake with dry-media Inlet Barrier Filter (IBF) and was performed with an Arriel 2C2 engine in turbojet configuration. Testing took place at the sea level ambient pressure Large Climatic Wind Tunnel (CWT) at Rail Tec Arsenal (RTA) in Vienna, Austria, by an integrated test team comprising engineers from the Royal Netherlands Aerospace Centre (NLR), Korea Aerospace Industries (KAI), and Safran Helicopter Engines. The test matrix covered the AC29-2C Appendix C 10,000 ft icing envelope, as well as simulated ground icing conditions, considering both a clean and artificially contaminated IBF. Beyond the aforementioned certification conditions, exploratory testing was performed in conditions with Supercooled Large Droplets (SLD) and rain. The test set-up consisted of the front section of the full-scale production cowling with internal modifications to accommodate the test engine and interface with the RTA exhaust gas handling system. Prior to tunnel entry, initial check-out and integration tests were performed with the same set-up at Safran, as well as in the Small CWT at RTA. Data gathering included the delta-pressure across the IBF, static pressures at the Aerodynamic Interface Plane (AIP), engine parameters, high-speed camera imagery, and 3-D scans of the critical ice shapes. The latter was used to support dry air flight testing with simulated ice shapes and blockage to demonstrate altitude effects and measure inlet distortion.

Introduction

Inlet Barrier Filters are finding increased application on rotorcraft engine air intakes as a means of passive protection of the engine against component degradation due to the ingestion of sand, dirt and other airborne particles. Despite their prevalence, scientific publications on the design and testing of IBF installations are sparse [1-5], particularly when it concerns the performance in icing conditions.

During operation, the IBF gradually collects contamination, causing a progressive increase in the inlet pressure loss and distortion. In most designs, cockpit annunciations cue the pilot at a set IBF blockage level to open an alternative airflow path that provides partial or total power recovery. IBF installations can be further subdivided into the categories of dry and oiled media systems, the latter relying on oil to ensure particle capture and retention, and prevent water absorption. Dry media filters, such as installed on the KAI LCH, achieve similar filtration efficiencies through tighter fiber structures at the expense of higher baseline pressure losses. The use of hydrophobic materials prevents water absorption, but due to the tight weave of the fibers, water retention may occur (ARP6901).

In 2016, the Federal Aviation Administration (FAA) issued a proposed Policy Statement with draft certification guidance for the evaluation of engine IBFs installed on rotorcraft. The document addresses the effects of IBF contamination and bypass operation on installed engine performance and operating characteristics, with a separate section dedicated to ice and snow protection. In turn, the SAE AC-9C committee is working on ARP6901 to establish industry recommended practices for the design and testing of passive rotorcraft engine (and APU) induction system ice protection, which includes the application of Inlet Barrier Filters.

Regardless of whether the applicant is seeking approval for flight into known icing, engine IBF installations must show compliance to the induction system ice protection regulations (§27.1093 and §29.1093). In the case of nonicing certified rotorcraft, the concept of limited exposure associated with escape from inadvertent icing encounters is typically applied. In the absence of an ice detection system, demonstration of a 30-minute hold in Appendix C Continuous Maximum (CM) icing conditions is deemed acceptable as per AC29.1093. Compliance demonstration typically involves icing wind tunnel testing of the induction system, with or without engine.

The Republic of Korea civil certification of the LCH has followed closely the FAA guidance and regulations in terms of engine induction system inadvertent icing qualification. The following details the full-scale sea level live-engine icing wind tunnel test activities performed to support compliance demonstration in advance of dry air simulated ice shape flight testing.

Description of Test Set-up

Testing in icing conditions was performed in the sea level pressure Large Climatic Wind Tunnel (CWT) at Rail Tec Arsenal (RTA) in Vienna, Austria. Figure 1 presents a schematic of the test section with installed contraction nozzle, enabling empty test section airspeeds up to 80 m/s. The test article is located in the test section area which is situated in the exhaust plume of the contraction nozzle. Despite the

unconventional set-up, the facility meets all requirements set forth in ARP5905 for the calibration and acceptance of icing wind tunnels.

In prior test activities of the engine air intake of the KAI KUH with electrothermal ice protection that was sensitive to impingement limits and water catch rate [6], dedicated CFD assessments were made to compare the air intake droplet collection efficiencies predicted for altitude-scaled wind tunnel test conditions against those computed for free flight. For the LCH test configuration, with unheated side mounted intakes, the scaling effects on impingement limits and water catch were not deemed as critical. Moreover, the live-engine test setup did not allow arbitrary scaling of the sea level engine volume flow to match the altitude conditions. As such, no corrections for altitude and wind tunnel installation effects were applied and the engine was run nominally at level flight power at sea level pressure. Variations in engine power up to Maximum Continuous Power were investigated at dedicated test points, including the 30-minute CM icing critical conditions.

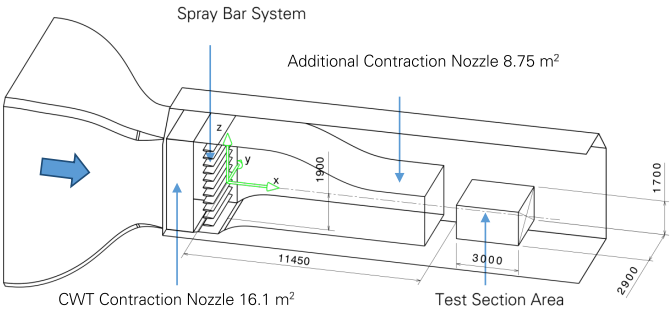

Figure 1. Schematic of RTA LCW indicating test section area in relation to contraction nozzle and spray bar system. Test section width and height equal 4.9 m and 5.9 m at minimum, respectively.

The test article shown in Figure 2 consists of the full-scale LCH engine cowling and Arriel 2C2 engine installed on the left-hand side, in turbojet configuration, supported by a set of metal frames to provide rigidity, angle of attack control and the elevation required to line up the intake with the icing spray center. The turbojet configuration of the test engine obviated the need for a water brake dynamometer for engine power absorption. A front fairing (magenta) has been added to the production cowling parts to reduce the ice accretions forming on the unprotected leading-edge of the truncated cowling (not present on the production aircraft). The left-hand engine air intake is protected by an interchangeable IBF.

The critical engine side is determined by the dry air installation losses as measured in flight test, which may differ between the left and right-hand side due to differences in, e.g., ram air pressure recovery or due to symmetric air intake swirl. In practice, with IBF installed the differences between the left and right hand engine installation losses are minimal. In the tunnel set-up, without main rotor wake swirl effects, asymmetry in intake ice accretion is driven by sideslip, which can be varied in either direction. As such, the decision to test the left hand engine is essentially arbitrary. However, any asymmetry in the sensitivity of the engines to IBF blockage due to icing must be determined through dry air flight testing with simulated blockage, including (post-icing) flight conditions not tested in the tunnel such as rearward flight.

A bypass door located on the upstream end of the intake cowling, shown in Figure 3, provides an alternate air path in case the pressure loss over the IBF exceeds the allowable threshold. The upstream location of the bypass enables substantial power recovery and exploits the presence of the plenum behind the IBF to minimize inlet distortion. The bypass is manually controlled by the pilot with the control panel indicating the level of blockage measured by the Delta-Pressure Sensor (DPS) on each intake. An external course-mesh Foreign Object Damage (FOD) screen over the bypass protects the engine from direct ice accretion and ingestion damage with open bypass. The exterior of the IBF features an additional bird strike protection screen, see also Figure 7. There are no further internal screens to protect the engine from ingestion damage.

The engine and related support equipment were designed and operated by Safran. The Arriel engine includes a 2-stage compressor, the first stage of which is situated immediately downstream a Bell mouth inlet duct that opens up into the plenum, shown in yellow in Figure 2. The engine is tested in turbojet configuration with the power turbine replaced by a fixed-diameter exhaust nozzle. The diameter has been defined such that the nozzle provides representative back pressure without the need for modulation with power setting. At moderate to high power settings the nozzle is chocked (M = 1). The engine exhaust was routed to the RTA water-cooled aspirated exhaust gas handling system through fixed stainless steel piping, leaving sufficient space around the engine exhaust nozzle to allow mixing of the hot exhaust gasses with cool ambient air from the test section. After cooling, the exhaust gasses are discharged outside of the tunnel circuit. In combination with the large cross section and length (>100 m) of the test section and the volume of air pass through it, no appreciable increase in ambient temperature was observed during engine operation. The initial testing in the Small CWT confirmed that the set-up did not affect the engine operation or performance compared to the engine test bench at Safran in which the test set-up and related instrumentation was first validated.

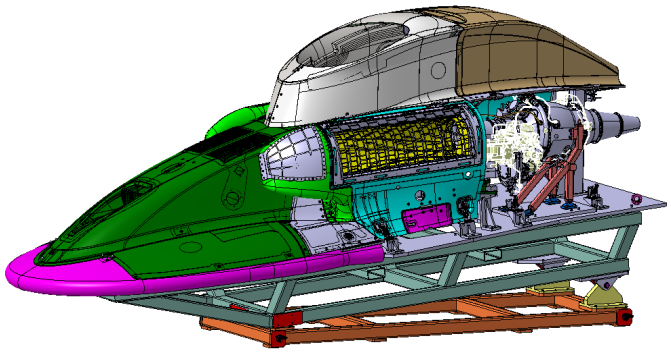

Figure 2. CAD rendering of LCH engine and air intake icing wind tunnel test rig excluding aft cowling section and exhaust gas handling interface.

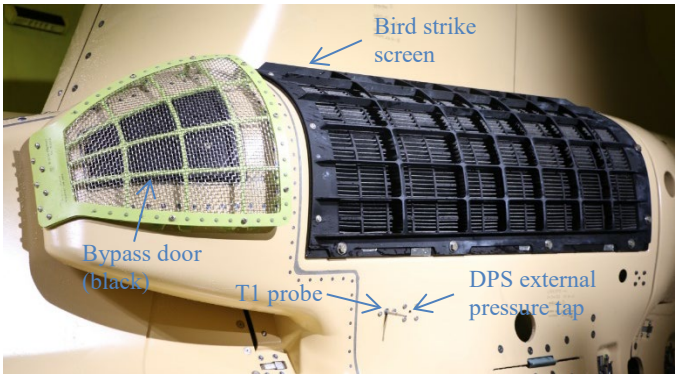

Figure 3. LCH engine air intake including IBF with bird strike screen and upstream bypass door with external FOD screen.

The delta-pressure across the IBF was measured using the production DPS, the upstream external port of which is indicated in Figure 3. Alternate external pressure ports were available as back-up in case ice accretion on the primary port was detected. The internal pressure port of the DPS is located in the plenum. A reference measurement was obtained by comparison of the static pressure upstream of the test article obtained at the exit of the contraction nozzle and the total pressure at the AIP. The latter was calculated from a local static measurement and computed velocity obtained from engine performance calculations, taking into account CFD-calculated duct loss between the IBF and the AIP. The static pressure at the AIP was obtained from static pressure ports distributed along the circumference of the inlet duct. The engine Installation and Operation Manual (IOM) limits on pressure loss are defined between the total pressure at the AIP and the static pressure upstream. The test set-up did not include an AIP rake for measuring inlet pressure and temperature distortion in comparison to IOM limits. These must be verified through dry air flight testing in which the IBF blockage is simulated in a manner analogous to the wind tunnel test, taking into account the blockage patterns observed in the tunnel. Lacking information on inlet flow distortion from the tunnel test activities, the simulated blockage may also be tuned to obtain maximum distortion effects [5].

Testing with artificially contaminated IBF was achieved by mounting a perforated metal plate on the back side of the removable IBF housing in a manner that avoided the risk of FOD damage due to, e.g, fasteners. This solution, shown in Figure 4, provided control of the pressure loss and the location of the blockage, without sensitivity to the external distribution of the unspecified contaminant in/on the pleats of the IBF. The uniform hole pattern was designed to achieve a pre-defined aggregate (IBF + plate) pressure loss at the target mass flow at the warmest static air temperature in the test matrix and sea level standard atmospheric pressure. The holes were partially taped to achieve a total IBF pressure loss with bypass closed equal to the cockpit annunciation blockage level at nominal operating conditions (not adjusted to test conditions). No constraints were defined for the pattern of the blockage and its influence on inlet flow distortion (not measured). The test points themselves were performed with bypass door open. Testing at intermediate blockage levels was not required by the authority.

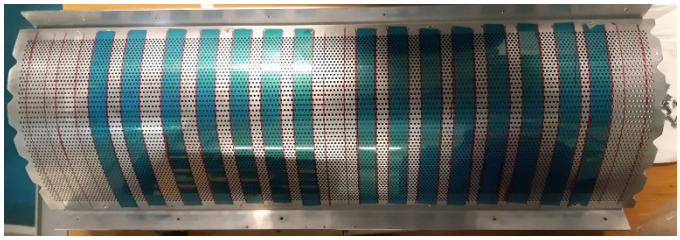

Figure 4. Perforated aluminum plate that was mounted onto the inner side of the IBF housing for contaminated IBF testing. The perforations are taped off to produce the targeted pressure loss with arbitrary distribution across the surface of the IBF.

Test Procedures

The integrated test team included engineers from NLR, KAI and Safran. NLR provided test director and icing certification specialist services. The engine piloting and assessment of engine operation was performed by Safran. KAI held the design organization responsibility as well as the decision making authority.

The majority of the test conditions corresponded to a 30-minute hold in Continuous Maximum (CM) icing conditions in accordance with AC29.1093 b(2)(ii)(B)(2) for an aircraft that does not feature an ice detector. Intermittent Maximum (IM) icing testing, though not required by the authority, consisted of a 30-min CM hold followed by a 5-min standard-distance IM cloud. In case the Liquid Water Content (LWC) limits of the RTA spray system were encountered for specific test conditions, the use of scaling based on accumulation parameter (through exposure time) was employed without regard for water catch rate and its effect on freezing fraction [7].

The engine gas generator speed (N1) was maintained throughout the icing exposure. As such, the mass flow and engine shaft power output reduces as the IBF pressure loss due to ice accretion builds up. To avoid the need for active compensation to approximate constant-power operation, the operating point in terms of target N1 and/or engine corrected mass flow was calculated for each test point assuming the maximum allowable IBF pressure loss. The rate of decrease of the engine mass flow thereby provides an indication of the icing impact on engine performance. If the derived engine corrected mass flow was not met at the target N1 prior to icing, the generator speed was increased to match the target mass flow. Note that due to this approach, the mass flow typically exceeded the target value.

The engine handling characteristics (surge and flameout) were verified immediately before and after icing exposure using a 3-SLAM procedure where engine power is cycled between flight idle and take-off power (TOP) in a manner similar to the procedure described in the recent update to EASA AMC 291093(b)(1)(i) (CS-29 Amd. 11). Unless engine parameter variations (continuously monitored) indicated otherwise, the critical condition for engine stability (as checked by 3-SLAM procedure) was presumed to occur at maximum icing exposure. Note that the 3-SLAM schedule was not modified to account for the reduction in surge margin with altitude. Dry air flight testing at altitude is required to demonstrate engine stability with representative simulated IBF blockage.

The following pass-fail criteria were defined:

1. No unacceptable variation in engine param. (N1, P3, T4, vibs)
2. No flame-out
3. No unacceptable compressor surge
4. No unacceptable mechanical damage
5. No exceedance of engine IOM limits
6. No internal ice accretion that forms engine ingestion risk

No pass-fail criteria were specified for inlet flow distortion (not measured); these aspects were addressed through subsequent dry air flight tests. The relevant engine parameters were monitored by Safran technicians throughout the test.

At the start of each icing test point, the potential presence of permanent degradation in engine performance due to mechanical damage incurred during the previous test point is checked by running two or more stabilized engine performance points at defined N1 and comparing with nominal conditions. A visual inspection of the 1st stage axial compressor was performed each time the IBF was replaced in between two test points. The 2nd stage centrifugal compressor can be inspected via borescope in case indications of ice ingestion are observed on the upstream axial compressor.

The margin of the measured inlet total pressure loss with respect to the engine IOM limits (converted to test power) were monitored

continuously by Safran technicians. This approach ensured that the IOM limit will not be exceeded within the operational power range of the engine, including during the acceleration to TOP as part of the slam procedure. In addition, built-in monitoring of predefined Do-Not-Exceed limits along with operator alerting protocols and automated engine spool-down provided additional protection against engine damage.

The initial test points were aimed at the identification of the critical static air temperature and drop size for the closed-bypass configuration, at the best climb speed (VY) and engine gas generator speed necessary for level flight assuming maximum allowable blockage. Variations in true airspeed (TAS) and power setting were considered to confirm the criticality of the low-speed condition with the bypass closed. In principle, the critical conditions were defined as those that, as per assessment by Safran technicians, produced the most adverse effects on engine performance, engine stability, and engine ice ingestion risk. Dedicated test points were performed around 0°C to check for potential downstream ice accretion in the plenum or on the engine inlet. The engine performance and operating characteristics were assessed throughout the icing exposure and through the 3-SLAM procedure at the end of each test point. As inlet pressure and temperature distortion were not measured, their influence could only be inferred from the observed engine characteristics. In the absence of discriminating effects on engine characteristics, the rate of increase in the IBF delta-pressure in combination with the ice accretions observed determined the criticality of the icing condition. In open-bypass configuration or in case of internal ice accretion, test condition criticality may instead be determined by engine ingestion risk.

Engineering Development Test Results

The certification test matrix was aimed at identifying the critical icing conditions within the constraints specified by the authority. As expected, the side-mounted air intake proved sensitive to droplet momentum effects, through drop size, airspeed, and power setting. No particular sensitivities were encountered in terms of engine performance or stability. Therefore, the critical closed-bypass icing conditions were defined by considering both IBF ice accretion and pressure loss. The highest pressure losses were found in the low-MVD range of the Appendix C envelope with the largest external ice accretions occurring at static air temperatures in the vicinity of -7.5°C. Although icing conditions around freezing, where a mixture of water and ice collected in between the IBF pleats, also resulted in considerable pressure loss, the potential for changes in severity due to parameter variations other than temperature was deemed greater at negative air temperatures. In light of these observations, the majority of the engineering test activities involved test parameter variations at a static air temperatures at and around -7.5°C. In practice, the dependence of the pressure loss on air temperature was found to be relatively small compared to the influence of drop size and airspeed. Additional testing was performed at the corners of the Appendix C envelope, including around freezing, to fully characterize the performance on the engine and intake in icing conditions.

Low Airspeed Icing

The minimum airspeed considered in the certification test matrix corresponded to the best climb speed (VY = 70 knots). To further explore the effect of level flight airspeed, engineering development tests were performed below V_{mini} at the minimum stable tunnel speed (40 knots) within ARP5905 specification at MVD = 15 µm. Figure 5 shows the effect of level flight airspeed and power for the critical clean-IBF bypass-closed icing condition at VY. It is apparent that, due to the droplet momentum effects at lower airspeed and higher power setting, ice accumulates over a larger streamwise extent of the IBF. Moreover, the shadowing effect of the IBF protector is notably reduced, leading to more substantial ice accretion on the filter itself and a correspondingly larger pressure loss. Conversely, the direct impingement ice accretion on the bypass door FOD screen, shown in Figure 6, is notably reduced at lower airspeed due to the limited streamline curvature and insensitivity to engine mass flow (with bypass door closed). The pressure loss due to icing is correspondingly largest at the lowest airspeed where also the proximity to the IOM pressure loss limit is smallest due to the higher power setting.

The importance of momentum effects was also apparent when comparing icing exposures at fixed LWC and decreasing MVD, which results in comparable ice thickness, but larger ice accretion area and, subsequently, a larger pressure loss across the IBF. That being said, the criticality is ultimately a balance between the cloud LWC, the distance travelled in-cloud, and the parameters that determine collection efficiency. This is exemplified by the fact that the critical airspeed at MVD = 20 µm was identified to be 70 knots.

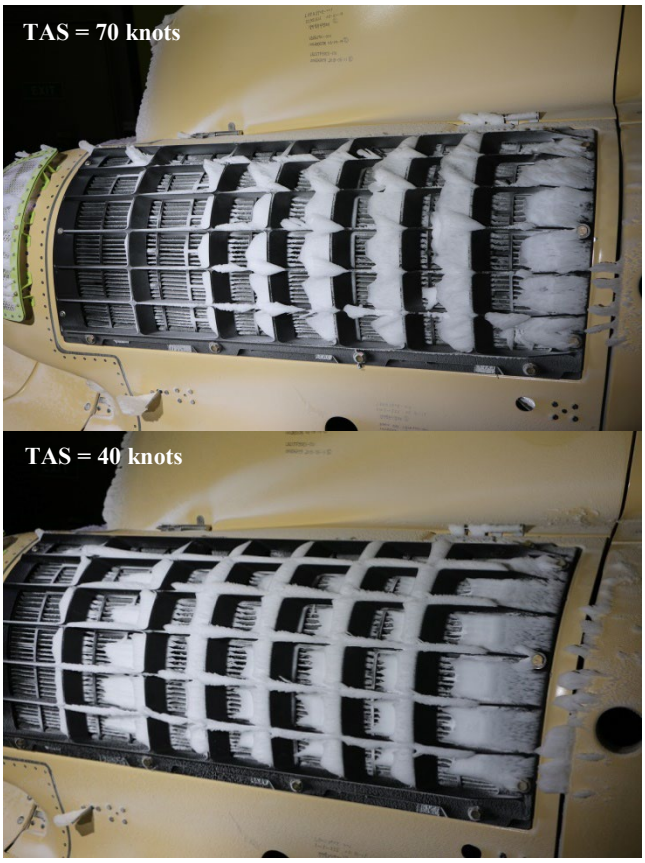

Figure 5. LCH engine air intake IBF and bird strike protection screen 30-minute ice shape at SAT = -7.5°C, MVD = 15 µm, LWC = 0.65 g/m^3.

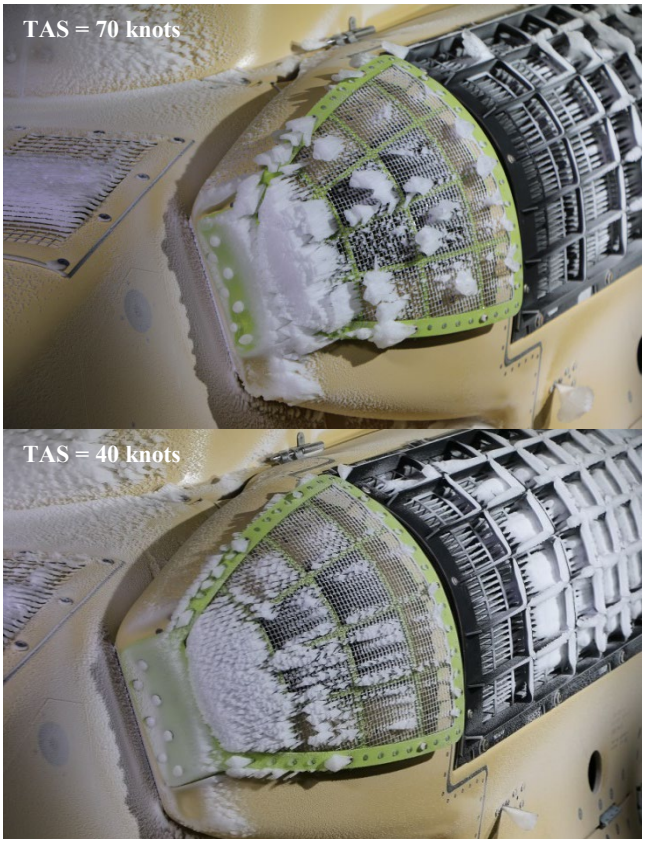

Figure 6. LCH engine air intake bypass FOD screen 30-minute ice shape at SAT = -7.5°C, MVD = 15 µm, LWC = 0.65 g/m^3 (bypass door closed).

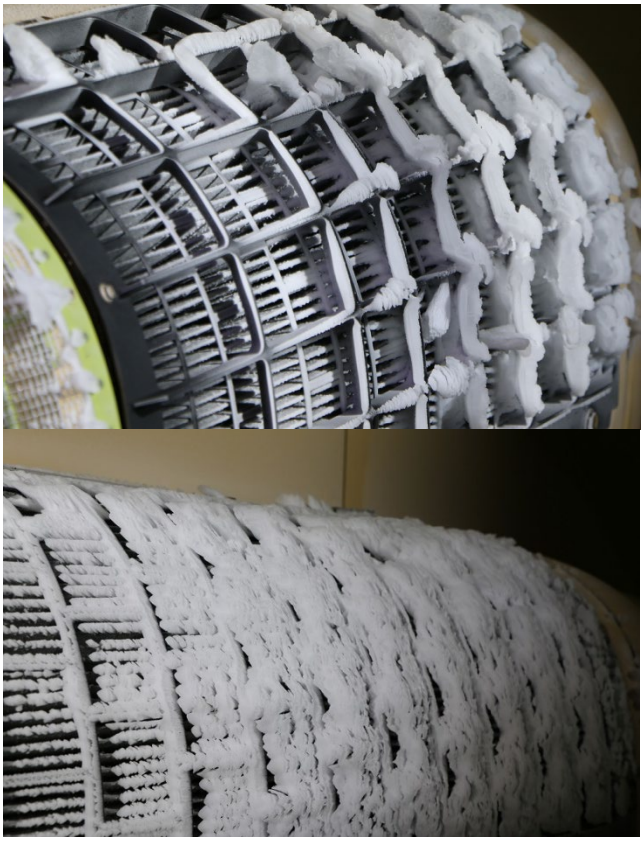

Figure 7. LCH engine air intake IBF with (top) and without (bottom) bird strike protection screen 30-minute 70 knots ice shape at SAT = -7.5°C, MVD = 15 µm, LWC = 0.65 g/m^3.

IBF Protector

To investigate the extent to which the aforementioned shadowing effect that was observed with the IBF bird strike protector installed was affecting the pressure loss across the IBF, repeat test points were performed without the protector. Figure 7 presents a close-up of the resulting 30-minute ice accretion for both configurations. The ice accreting on the IBF protector is scallop-like in appearance, reflecting the effective sweep angle of the surface relative to the drop trajectories. The scallops are oriented in the direction of the local airflow and generate comparatively little pressure loss (at least for the steady flight condition in which the ice was accreted). Moreover, the air downstream of the IBF protector is depleted of water droplets, resulting in reduced ice accretion on the IBF filter pleats. By comparison, the ice accretion on the clean IBF on the bottom of Figure 7 shows a substantially larger iced extent of the filter. Nevertheless, and somewhat surprisingly, the rate of increase in the pressure loss measured at the AIP was nearly identical for both configurations. Upon closer inspection of the ice accreted on the clean IBF, it is apparent that also here scallop ice forms, in this case on the tips of the streamwise-oriented pleats of the filter, allowing air to pass through with relatively benign pressure loss. A single test was run in the same conditions as reported in Figure 7 but for a duration of 120 minutes without cloud-extent scaling, starting with a clean filter and with protector installed. The test resulted in substantial ice accretion on the IBF protector, a pressure loss that still remained below the blockage limit, but with a rate of increase that roughly doubled after 80 minutes in icing and showing no sign of stabilization. Nevertheless, the IBF without protector installed would likely have fared worse.

Contaminated IBF

Numerous test conditions were repeated with simulated IBF contamination. The blockage was iteratively tuned in dry air at the target tunnel velocity and engine speed using the aircraft DPS. Ultimately, this resulted in 52% of the perforated plate holes being blocked by tape. The engine gas generator speed N1 was increased as needed to achieve the target air intake flow rate. The comparison Figure 8 reveals a higher collection efficiency of the upstream part of the contaminated IBF due to the redistribution of the air flow through the filter, biased towards the front. The changes in the streamlines were also apparent on the FOD screen, which showed more ice accretion on the downstream end (close to the upstream end of the IBF). The rate of increase in the pressure loss due to icing was not notably affected by the simulated filter contamination. This is not entirely surprising given the fact that the contamination was applied fairly uniformly for this test. Physical contamination with particulates on the outside of the filter (in between the pleats, potentially non-uniformly distributed) may produce slightly different results.

Figure 8. LCH engine air intake IBF with and without simulated contamination 30-minute 70 knots ice shape at SAT = -7.5°C, MVD = 15 µm, LWC = 0.65 g/m^3.

Figure 9. LCH engine air intake IBF and bypass FOD screen 30-minute 70 knots ice shape at SAT = -7.5°C, MVD = 15 µm, LWC = 0.72 g/m^3 with open bypass.

Open Bypass Testing

Testing with open bypass was gradually extended to minimize the risk of engine damage due to ice ingestion. Part of the testing was performed with an additional internal FOD screen at the bell mouth upstream of the AIP. The internal FOD screen served purely as a risk mitigation for the test and was removed on later test points. In initial tests the bypass was opened for about 5 minutes following a 15 minutes icing encounter with the bypass closed. After shutdown and visual inspection of the plenum and the compressor face, the test was restarted. Figure 9 shows the ice accretion on the IBF and bypass FOD screen following a 30-minute exposure with the bypass door open. In comparison to previous test points with the bypass door closed, the ice accretion on the IBF is slightly reduced. However, the extent and thickness of the ice accretion on the external FOD screen is significantly larger. The impact of the external FOD screen ice on the air intake pressure loss remains relatively benign due to the alternative flow path that is available through the largely unobstructed IBF. Due to the extent of FOD screen relative to the size of the bypass and the small standoff distance, the ice on the FOD screen does not represent an engine ingestion hazard. This was confirmed through power and wind-on warm-up testing to document shed ice trajectories.

Supercooled Large Droplets (SLD)

Noting the sensitivity to droplet momentum effects, favoring higher pressure loss for smaller drop size, a single test condition was run with drops in the SLD size spectrum (not a certification requirement for rotorcraft). In the interest of time, the test was conducted for freezing drizzle conditions, which can be produced with the standard spray bar system [8]. For freezing rain conditions dedicated SLD nozzles must be installed [9]. The LWC far exceeded the Appendix O envelope (0.4 g/m^3 at -7.5°C). The icing time was correspondingly scaled to achieve an exposure equivalent to a standard cloud extent of 17.4 nm. As the intention was not to reproduce exact Appendix O SLD conditions, but rather to obtain an indication of the sensitivity to droplets in the SLD size spectrum, no other scaling considerations were applied. The resulting 30-minute 70 knots ice accretion is shown in Figure 10. The large momentum of the SLD droplets dominates the droplet trajectory. The trajectories are barely affected by the pressure gradients around the aircraft, leading to high collection efficiencies at stagnation surfaces directly exposed to the flow, like the external FOD screen. After impacting the FOD screen, the relatively large water droplets freeze, with some delay, to form the observed glaze ice. In contrast, even with the bypass closed, almost no ice accretion is visible on the IBF where the pressure gradients due to the mass flow through the engine are insufficient to deflect the high-inertia droplets from their straight-line trajectories. Accordingly, the pressure loss due to icing remained negligible throughout the icing encounter.

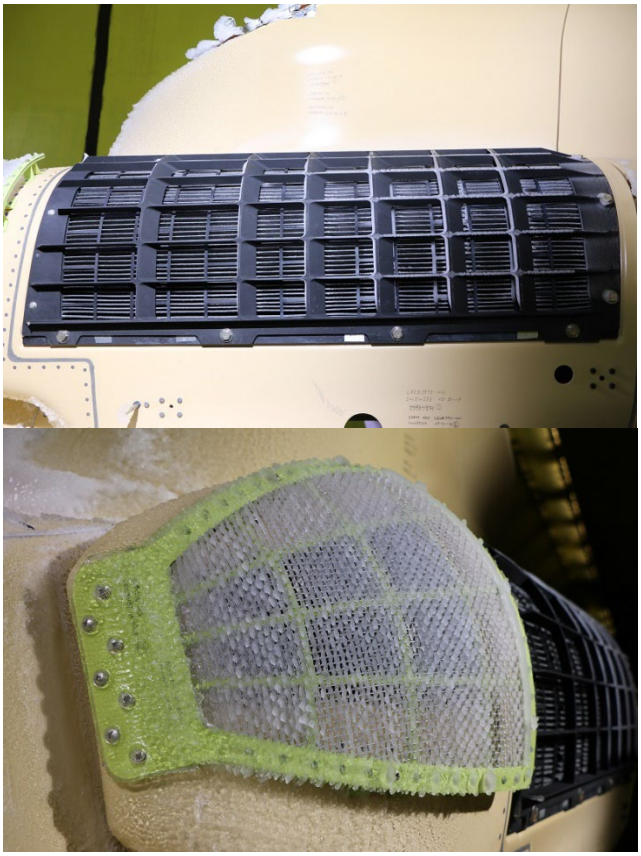

Figure 10. LCH engine air intake IBF and bypass FOD screen 30-minute 70 knots ice shape at SAT = -7.5°C, MVD = 100 µm, LWC = 0.72 g/m^3.

Wet IBF Testing

Issues have been reported with dry-media IBF installations that have been left parked outside without rain cover where subsequent engine power application during take-off in heavy rain is believed to have caused engine damage due to ingestion of a surge of water from the saturated filters, prompting an FAA Airworthiness Directive for certain aircraft models while the issue remains under investigation. Though above-freezing rain or water cloud testing was not foreseen at the outset of the test campaign, a test condition was improvised using the icing spray bar system to generate a water droplet cloud at the highest achievable LWC and MVD (well beyond the system calibration range) and starting with a pre-soaked IBF. The intent was not to replicate a specific atmospheric or high-MVD precipitation condition, but to thoroughly wet the IBF both prior to engine start and during testing. The test was run for 30 minutes at minimum tunnel speed to show stabilization of the pressure loss as shown in Figure 11. Despite a relatively aggressive engine startup protocol, no issues were encountered due to rapid ingestion of water by the compressor. The pressure loss due to filter (re)saturation builds up quickly and subsequently remains stable below the cockpit annunciation threshold. The pressure loss accumulated with bypass open is remarkably close to the condition with bypass closed. Post-test inspection confirmed that there was no damage to the compressor and that there was no accumulation of water in the plenum that could cause an engine ingestion risk upon freezing.

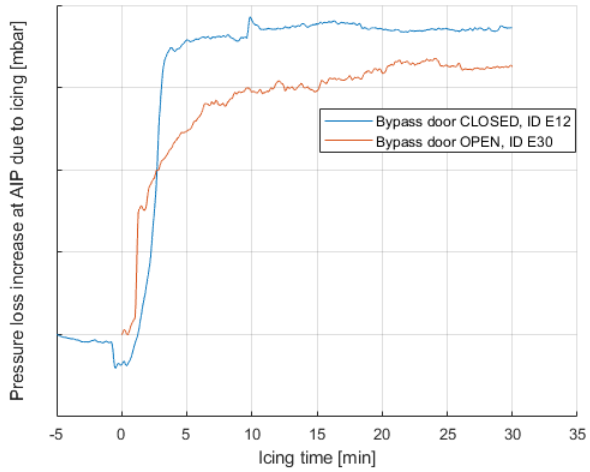

Figure 11. Increase in total pressure loss between free stream and the AIP due to simulated above-freezing liquid cloud conditions with LWC = 4.5 g/m^3 and MVD = 50 µm.

Conclusions & outlook

The live-engine icing wind tunnel test activities described herein provided the KAI design team with valuable engineering data beyond what was required for certification purposes. The rate of increase in the total pressure losses due to Appendix C ice accretion on the IBF were observed to be such that, even starting with a substantially contaminated filter, the delta-pressure remains far removed from the IOM pressure loss and IBF structural limits for inadvertent CM icing encounters up to 30 minutes.

Dry air flight testing with simulated ice shapes and/or artificial blockage of the IBF is necessary to demonstrate acceptable engine operation at altitude along with documentation of measure inlet distortion. In flight test, artificial blockage of the IBF can be achieved by similar means as those employed in the wind tunnel. CAD data from 3-D scans of the iced wind tunnel test article such as shown in Figure 12 can be used to define simulated ice shapes if deemed necessary.

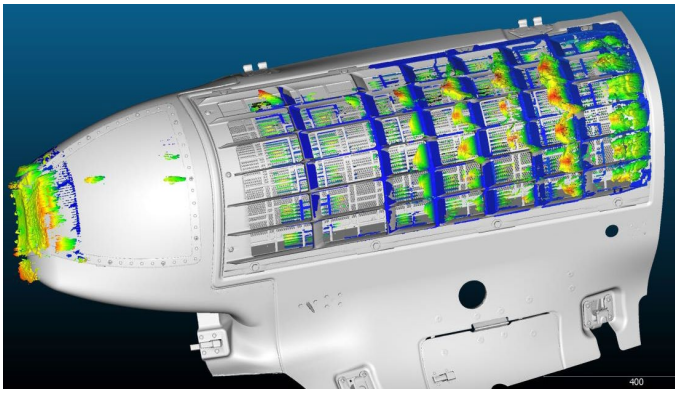

Figure 12. 3-D scan of 70 knots 30-minute CM ice accretion at SAT = -7.5°C, MVD = 15 µm , courtesy of Austrian Institute for Icing Sciences (AIIS).

References

1. Ockier, C., Müller, H., Linke, W., Kolb, C. et al., "Flight Testing an Engine Inlet Barrier Filter for the EC145", presented at the American Helicopter Society 65th Annual Forum, USA, May 27-29, 2009.
2. Simpson, D. and Piñero, E., "Overview of the Engine Inlet Barrier Filter Flight Test Efforts on the V-22", presented at the American Helicopter Society 71st Annual Forum, USA, May 5-7, 2015.
3. Hwa, V., "Test and Evaluation of an Inlet Barrier Filter to Increase Engine Time-On-Wing for the Bell Boeing V-22 Osprey Tiltrotor", MSc thesis, University of Texas, May, 2015.
4. Bodjo, N. and Filippone, A., "Performance Prediction of Inlet Barrier Filter Systems for Rotorcraft Engines", *Journal of Aircraft*, 48(6):1903-1912, 2011, doi:10.2514/1.C031335.
5. Aubert, R., "Installation and Certification of IBF for Inadvertent and Known Icing", SAE AC9C, October, 2019.
6. Lammers, K., Van 't Hoff, S.C., Ferschitz, H. and Wannemacher M., "Helicopter Engine Air Intake Icing Wind Tunnel Certification Test", presented at 44th European Rotorcraft Forum, The Netherlands, September 18-21, 2018.
7. D.N. Anderson, "Manual of Scaling Methods", NASA/CR-2004-212875, March, 2004.
8. Breitfuß, W. *et al.* 'Project WP6 SLD test capabilities RTA calibration results´ Public workshop ICE-GENESIS H2020, 2022.
9. Ferschitz, H. *et al.* 'Development of SLD Capabilities in the RTA Icing Wind Tunnel', *SAE International Journal of Aerospace*, 10(1), pp. 12–21, 2017.

Contact Information

Stefan van 't Hoff, NLR: Stefan.van.t.Hoff@nlr.nl, +31(0)652762907.

Acknowledgments

The authors hereby acknowledge the valuable support provided by the remainder of the test team members and in particular the guidance provided by D.C. Parkins and C. Greenberg.

Definitions/Abbreviations

AIP	aerodynamic interface plane
ARP	aerospace recommended practice
CM	continuous maximum
DPS	delta pressure sensor
IBF	inlet barrier filter
IM	intermittent maximum
IOM	installation & operation manual
FOD	foreign object damage
LWC	liquid water content
MVD	median volume diameter
N1	gas generator speed
P3	compressor exit pressure
SAT	static air temperature
SLD	supercooled large droplets
T4	turbine outlet temperature
TAS	true airspeed
TOP	take-off power
VY	best climb speed